

Report No.
UCB/SEMM-2015/02

Structural Engineering
Mechanics and Materials

**Thermal Phase Transformations in
Commercial Dental Files**

By

Rajiv G. Govindjee and Sanjay Govindjee

July 2015

Department of Civil and Environmental Engineering
University of California, Berkeley

Thermal Phase Transformations in Commercial Dental Files

Rajiv Govindjee & Sanjay Govindjee*
University of California, Berkeley

July 21, 2015

Abstract

This brief note reports upon an experimental study of thermal phase transitions in commercial dental files. Five files (HyFlex CM, ProTaper Next, ProTaper Universal, TRUShape, and Vortex Blue) were sectioned and tested via differential scanning calorimetry (DSC) with scans ranging from approximately ± 60 °C. All files were found to have homogeneous thermal transitions as a function of axial coordinate and were seen to be thermally stable (displayed repeatable DSC scans) over several cycles. The different files however displayed a wide range of behaviors with varying transformation temperatures and different solid-solid phase transformations. Some presented classical austenite to martensite, presumably cubic to monoclinic, and the reverse. Others however included apparent intermediate phases, presumably R-phase (rhombohedral) structures.

1 Materials and Methods

1.1 Materials

Five NiTi dental files were tested (HyFlex CM, ProTaper Next, Protaper Universal, TRUShape, and Vortex Blue), with two samples from each file being tested. To prepare the samples, multiple sections of 1mm to 4 mm were

*E-mail: s.g@berkeley.edu

cut from each file using manual diagonal cutters and weighed to an accuracy of ± 0.01 mg before being placed in an Tzero aluminum pan (also weighed to an accuracy ± 0.01 mg) and non-hermetically sealed. Samples were prepared starting at the file tip in short sections with the aim of achieving a total sample weight of approximately 10 to 20 mg.

1.2 Methods

Each sample was placed in a TA Instruments Q2000 differential scanning calorimetry (DSC) instrument (calibrated with indium) along with an empty Tzero aluminum reference pan. The purge gas used was nitrogen, at a flow rate of 50 ml/min. The samples were first heated to 60 °C, then cooled to -60 °C at a rate of -10 °C/min, followed immediately by a heating cycle at 10 °C/min up to 60 °C. The heating/cooling cycle was performed three times per sample. Some samples were cycled at ± 90 °C instead, as their transformations occurred at more extreme temperatures.

2 Analysis

All data was analyzed using TA Instrument's Universal Analysis software. The start and finishing temperatures were determined as the intersection of the line tangent to the curve at its point of inflection and the baseline. Baselines were selected using TA Instrument's sigmoidal tangent method (selecting 4 points).

2.1 ProTaper Universal

The ProTaper Universal file displayed a classic austenite-martensite (presumably cubic-monoclinic) phase transformation centered close to 0 °C. Sample 1 was very repeatable over all 3 cool-heat cycles; however Sample 2 displayed some signs of functional fatigue during cycling. Numerical values can be found in Table 1. For Sample 1 only one scan is shown in Fig. 1. For Sample 2, all three scans are shown and demonstrate the functional fatigue during thermal cycling; see Figs. 2-4.

2.2 ProTaper Next

The ProTaper Next file displayed a classic austenite-martensite (presumably cubic-monoclinic) phase transformation centered close to body temperature. Sample 1 was very repeatable over all 3 cool-heat cycles; however Sample 2 displayed slight signs of functional fatigue during cycling. Numerical values can be found in Table 2. For Sample 1 only one scan is shown in Fig. 5. For Sample 2, all three scans are shown and indicate some functional fatigue during thermal cycling; see Figs. 6-8.

2.3 Vortex Blue

The Vortex Blue file displayed classic R-phase transformations. Upon cooling, an austenite (presumably cubic) to R-phase (presumably rhombohedral) occurred at roughly 30 °C. An R-phase to martensite (presumably monoclinic) took place upon further cooling around -60 °C. Upon heating the $M \rightarrow R$ transformation around 20 °C precedes the $R \rightarrow A$ transformation which takes place around 30 °C. Numerical values can be found in Table 3. For Sample 1 only one scan is shown in Fig. 9. For Sample 2, a full scan is shown as well as two zoom in scans; see Figs. 10-12. Looking at Fig. 12 shows the low temperature $R \rightarrow M$ transformation which can only be partially captured due to limitations of the instrumentation. The initiation occurs around -42.82 °C but it is not clear that it has completed before -90 °C where the cycle reversed. The second cycle for Sample 2 is shown in Fig. 13.

2.4 HyFlex CM

The HyFlex CM file displayed classic R-phase transformations. Upon cooling, the austenite (presumably cubic) transforms to an R-phase (presumably rhombohedral) just below 20 °C. There is then a wide R-phase to martensite (presumably monoclinic) well below 0 °C. During heating the $M \rightarrow R$ and $R \rightarrow A$ transformations overlap and can not be separated. Numerical values can be found in Table 4. DSC traces for the two samples which were fully repeatable are shown in Figs. 14 and 15.

2.5 TRUShape

The TRUShape file displayed classic R-phase transformations. However, upon both the cooling and heating cycles the R-phase and the martensitic transformation overlap each other and can not be separated in terms of transformation temperature. Numerical values can be found in Table 5. DSC traces for the two samples are shown in Figs. 16-18. Sample 2 showed a small amount of functional fatigue under thermal cycling.

3 Tables

Table 1: ProTaper Universal

	$M_s(^{\circ}\text{C})$	$M_f(^{\circ}\text{C})$	$\Delta H_{A \rightarrow M}(\text{J/g})$	$A_s(^{\circ}\text{C})$	$A_f(^{\circ}\text{C})$	$\Delta H_{M \rightarrow A}(\text{J/g})$
Sample 1	9.40	-9.32	1.127	-5.10	11.36	1.847
Sample 2, Cycle 1	9.37	-7.44	1.072	-4.61	10.64	1.272
Sample 2, Cycle 2	9.12	-6.99	1.074	-4.33	9.72	1.118
Sample 2, Cycle 3	8.98	-6.93	1.107	-4.40	10.24	1.230
Mean	9.2	-7.7	1.10	-4.6	10.5	1.4
Std. Dev.	0.2	1.1	0.03	0.3	0.7	0.3

Table 2: ProTaper Next

	$M_s(^{\circ}\text{C})$	$M_f(^{\circ}\text{C})$	$\Delta H_{A \rightarrow M}(\text{J/g})$	$A_s(^{\circ}\text{C})$	$A_f(^{\circ}\text{C})$	$\Delta H_{M \rightarrow A}(\text{J/g})$
Sample 1	44.61	26.22	1.432	30.52	45.72	1.094
Sample 2, Cycle 1	43.86	10.63	2.097	29.41	52.66	1.199
Sample 2, Cycle 2	43.63	12.29	1.791	29.12	51.41	1.279
Sample 2, Cycle 3	43.55	11.46	1.971	28.63	52.99	1.303
Mean	43.9	15	1.8	29.4	50	1.22
Std. Dev.	0.5	7	0.3	0.8	3	0.09

Table 3: Vortex Blue

	$R_s(^{\circ}\text{C})$	$R_f(^{\circ}\text{C})$	$\Delta H_{A \rightarrow R}(\text{J/g})$	$RR_s(^{\circ}\text{C})$	$RR_f(^{\circ}\text{C})$	$\Delta H_{M \rightarrow R}(\text{J/g})$
Sample 1	30.69	26.55	3.219	16.26	26.40	1.246
Sample 2, Cycle 1	31.38	27.21	2.956	11.46	25.61	3.764
Sample 2, Cycle 2	31.35	27.27	2.881	15.96	25.89	1.025
Mean	31.14	27.0	3.02	15	26.0	2.0
Std. Dev.	0.4	0.4	0.19	2	0.4	1.5
	$A_s(^{\circ}\text{C})$	$A_f(^{\circ}\text{C})$	$\Delta H_{R \rightarrow A}(\text{J/g})$			
Sample 1	30.81	33.85	2.418			
Sample 2, Cycle 1	30.89	33.61	2.118			
Sample 2, Cycle 2	30.73	33.66	2.225			
Mean	30.81	33.71	2.25			
Std. Dev.	0.08	0.13	0.15			

Table 4: HyFlex CM

	$R_s(^{\circ}\text{C})$	$R_f(^{\circ}\text{C})$	$\Delta H_{A \rightarrow R}(\text{J/g})$	$M_s(^{\circ}\text{C})$	$M_f(^{\circ}\text{C})$	$\Delta H_{R \rightarrow M}(\text{J/g})$
Sample 1	21.39	17.47	3.260	-8.61	-31.36	4.627
Sample 2	21.49	16.51	3.862	-2.01	-33.20	6.530
Mean	21.44	16.99	3.56	-5	-32.3	5.6
Std. Dev.	0.07	0.68	0.43	5	1.3	1.4
	$A_s(^{\circ}\text{C})$	$A_f(^{\circ}\text{C})$	$\Delta H_{MR \rightarrow A}(\text{J/g})$			
Sample 1	20.27	43.04	14.13			
Sample 2	22.73	43.96	14.69			
Mean	21.5	43.5	14.4			
Std. Dev.	1.7	0.7	0.4			

Table 5: TRUShape

	$M_s(^{\circ}\text{C})$	$M_f(^{\circ}\text{C})$	$\Delta H_{A \rightarrow R \rightarrow M}(\text{J/g})$	$A_s(^{\circ}\text{C})$	$A_f(^{\circ}\text{C})$	$\Delta H_{M \rightarrow R \rightarrow A}(\text{J/g})$
Sample 1	24.91	15.87	2.586	18.57	27.04	2.323
Sample 2, Cycle 1	32.54	22.68	2.941	25.05	34.03	2.626
Sample 2, Cycle 2	32.57	22.57	3.008	24.99	33.92	2.505
Mean	30	20	2.8	22	31	2.49
Std. Dev.	4	4	0.2	4	4	0.15

4 Figures

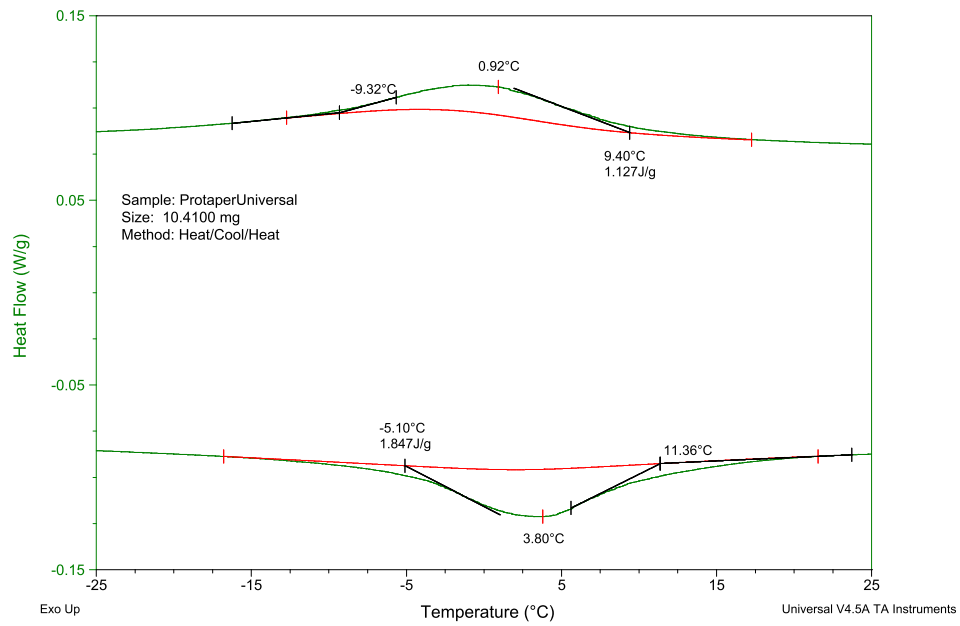


Figure 1: ProTaper Universal, Sample 1

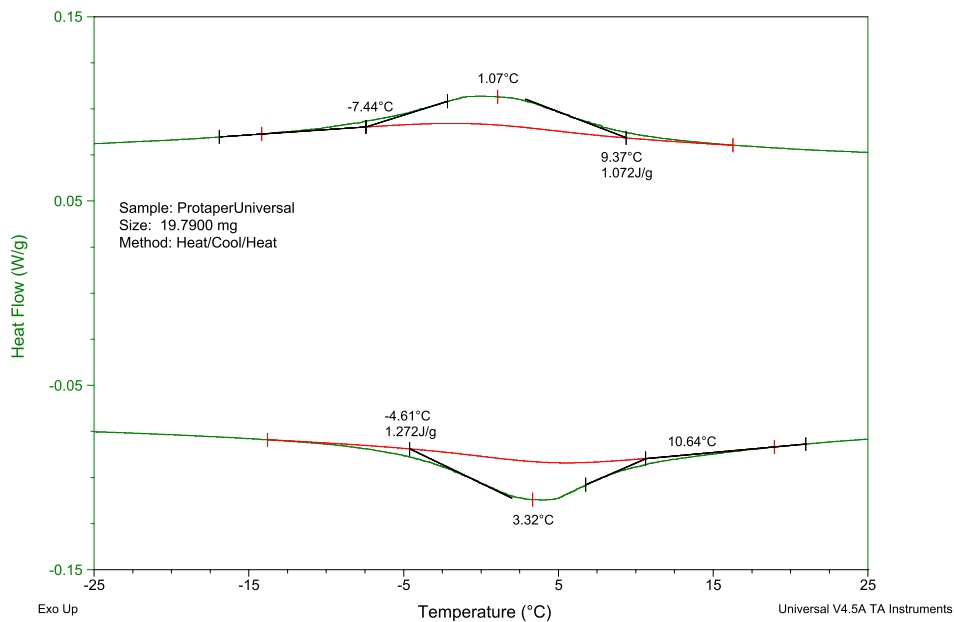


Figure 2: ProTaper Universal, Sample 2, Cycle 1

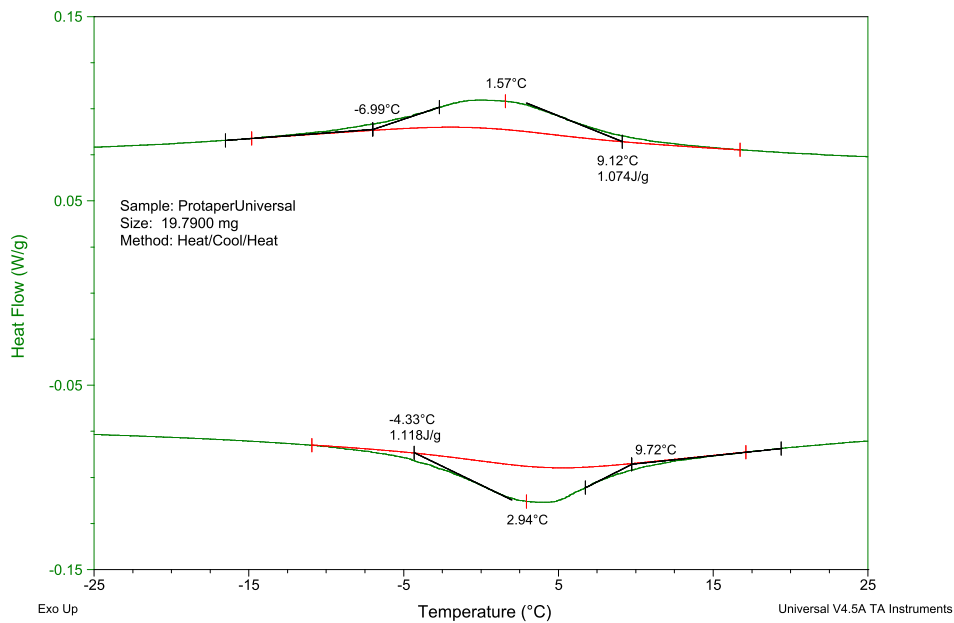


Figure 3: ProTaper Universal, Sample 2, Cycle 2

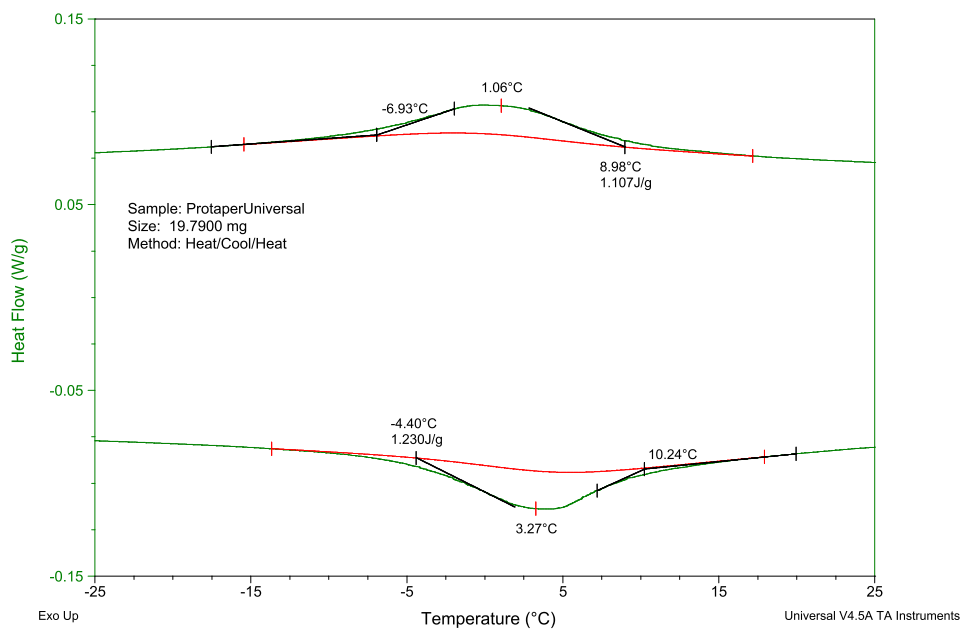


Figure 4: ProTaper Universal, Sample 2, Cycle 3

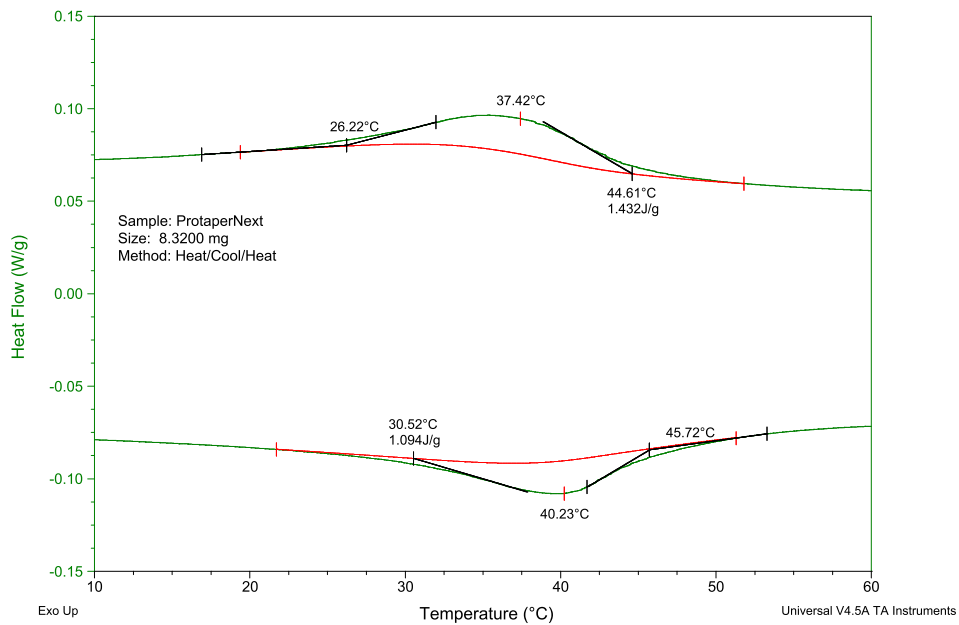


Figure 5: ProTaper Next, Sample 1

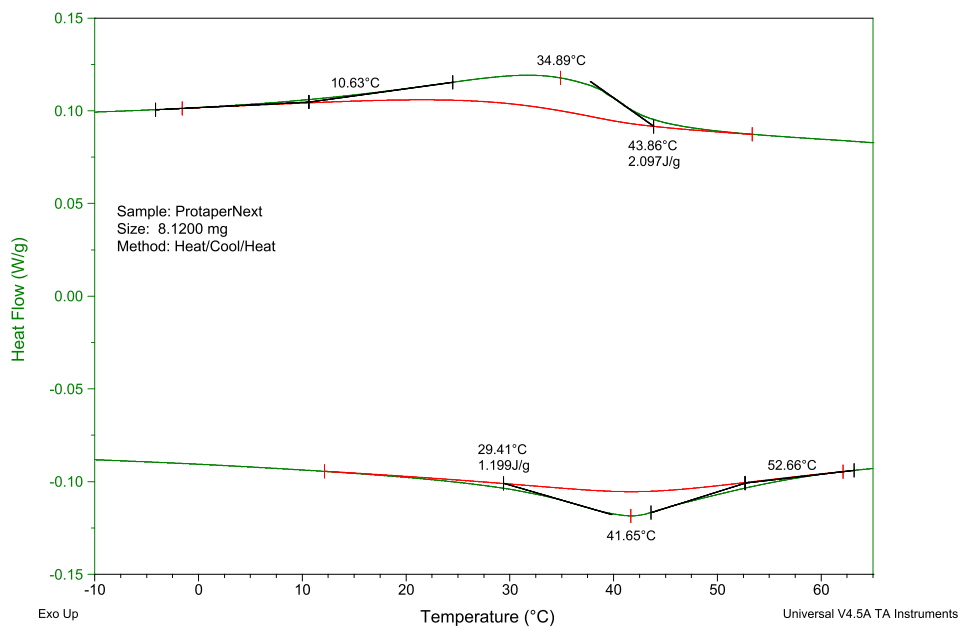


Figure 6: ProTaper Next, Sample 2, Cycle 1

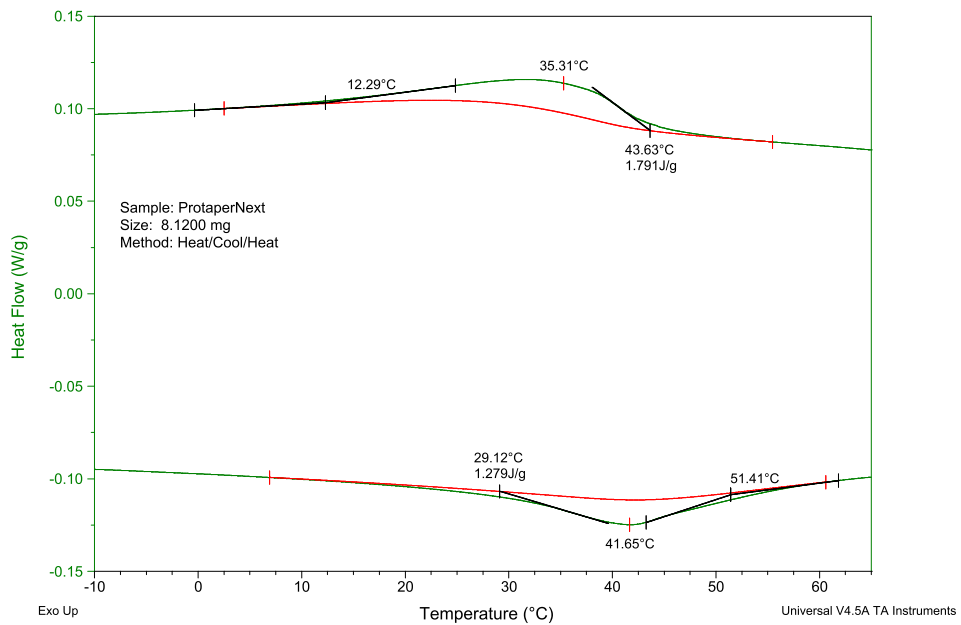


Figure 7: ProTaper Next, Sample 2, Cycle 2

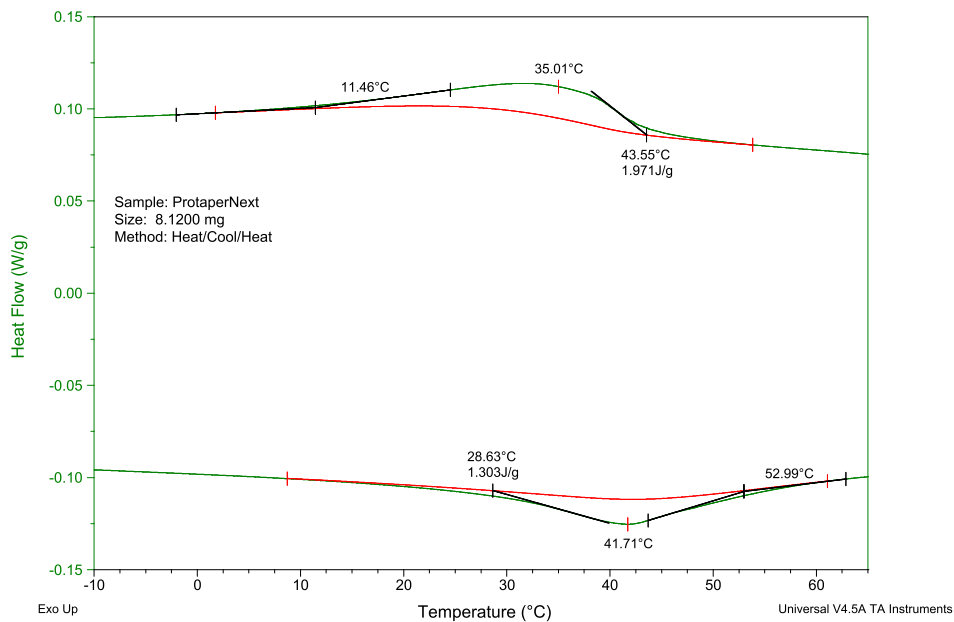


Figure 8: ProTaper Next, Sample 2, Cycle 3

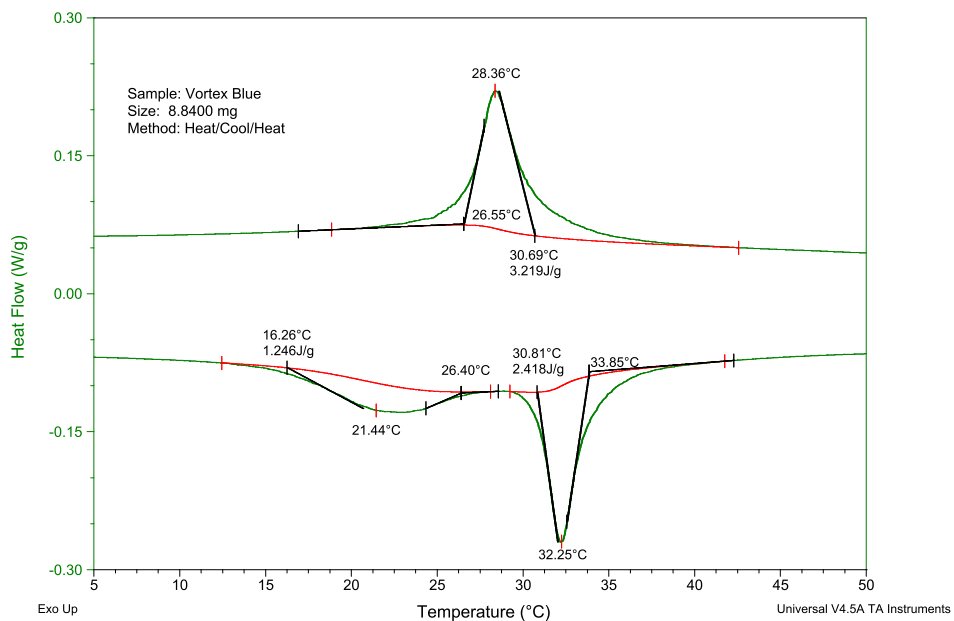


Figure 9: Vortex Blue, Sample 1

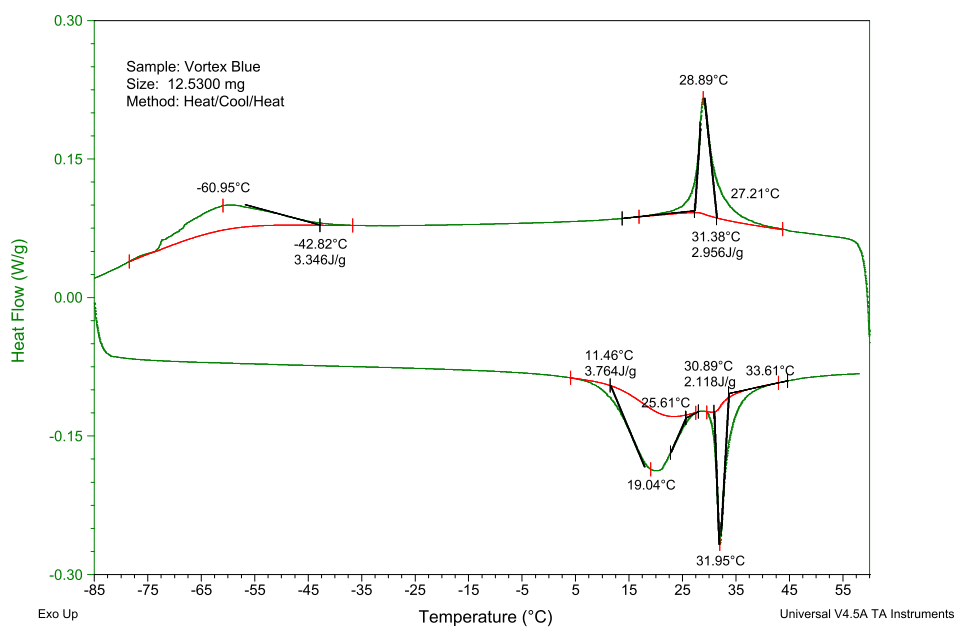


Figure 10: Vortex Blue, Sample 2

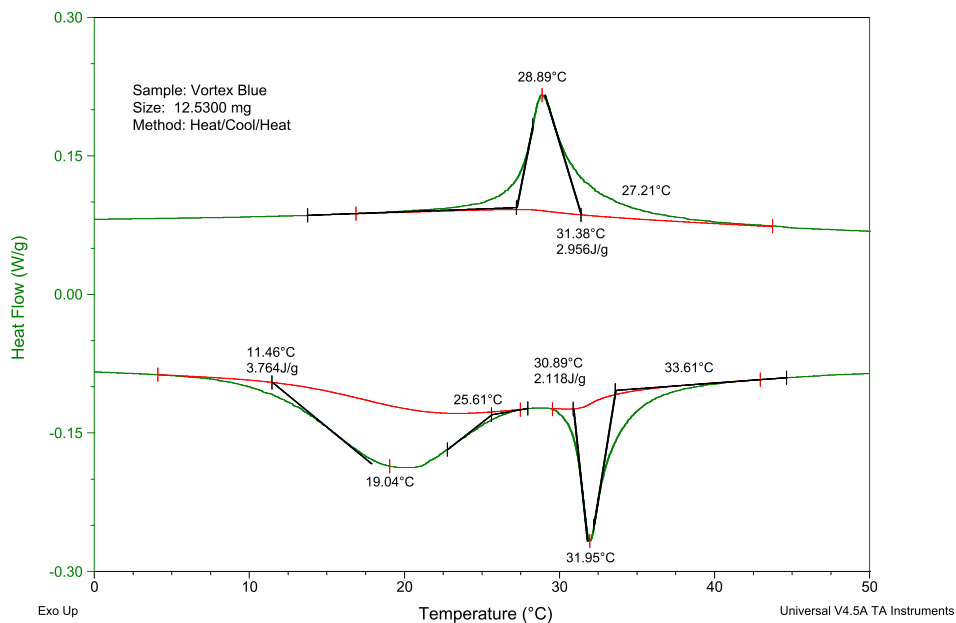


Figure 11: Vortex Blue, Sample 2, $R \rightarrow A$ zoom, Cycle 1

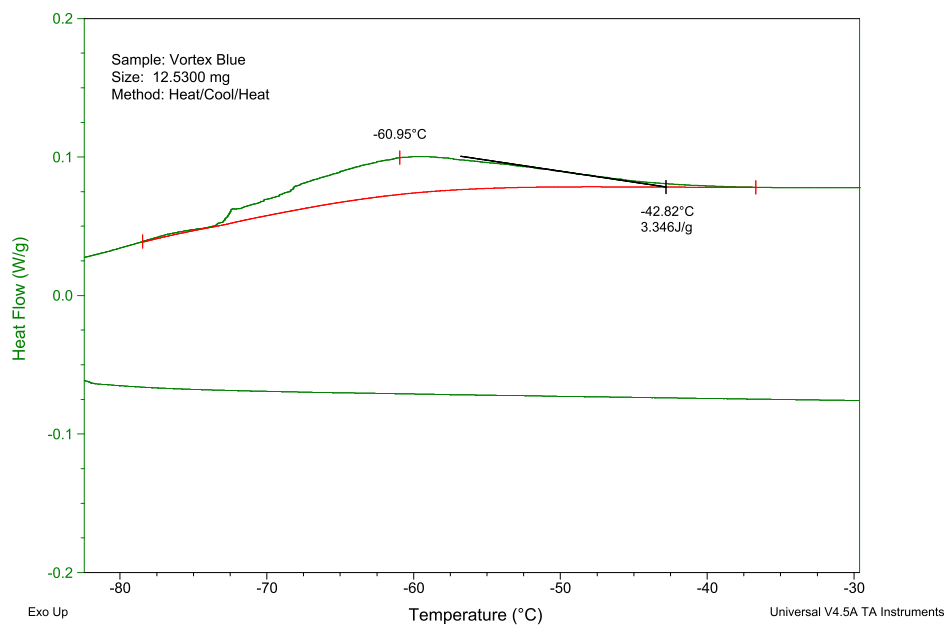


Figure 12: Vortex Blue, Sample 2, $R \rightarrow M$ zoom, Cycle 1

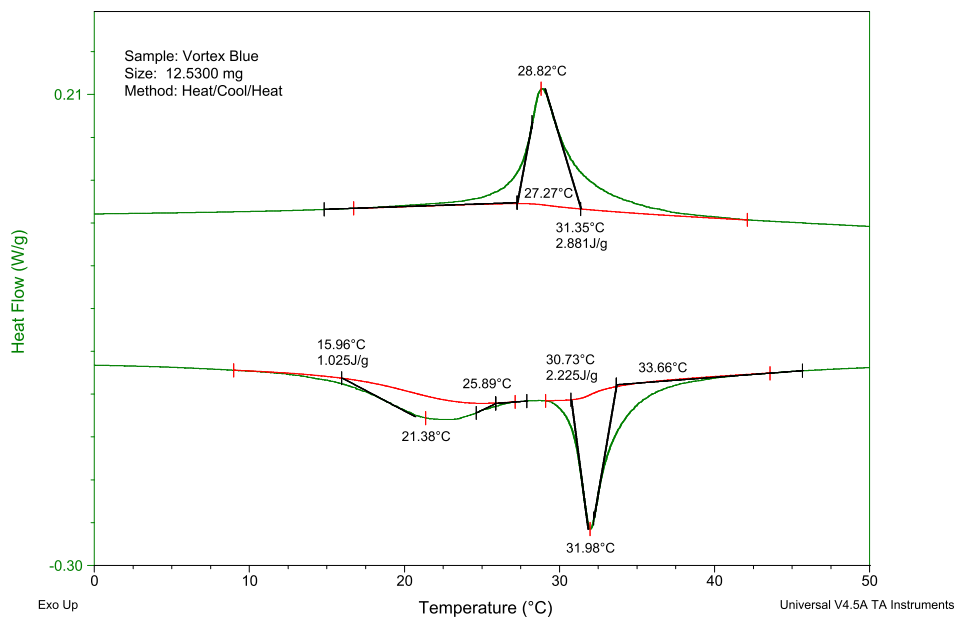


Figure 13: Vortex Blue, Sample 2, Cycle 2

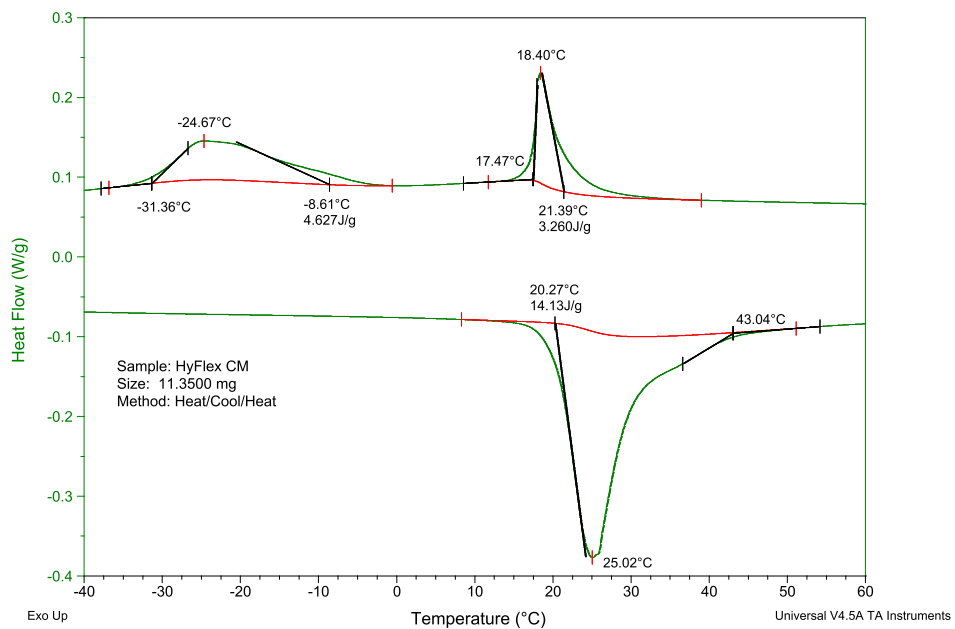


Figure 14: HyFlex CM, Sample 1

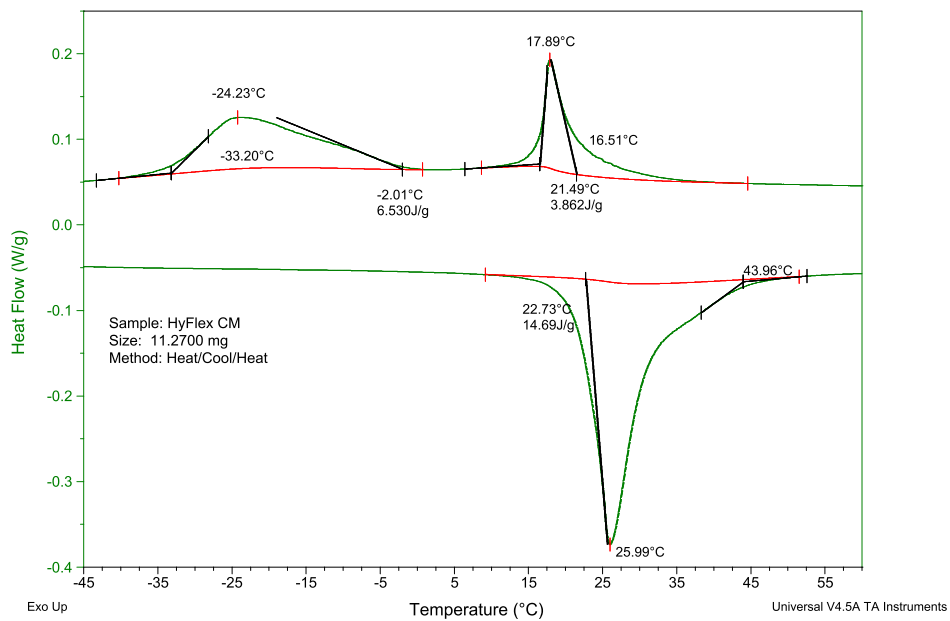


Figure 15: HyFlex CM, Sample 2

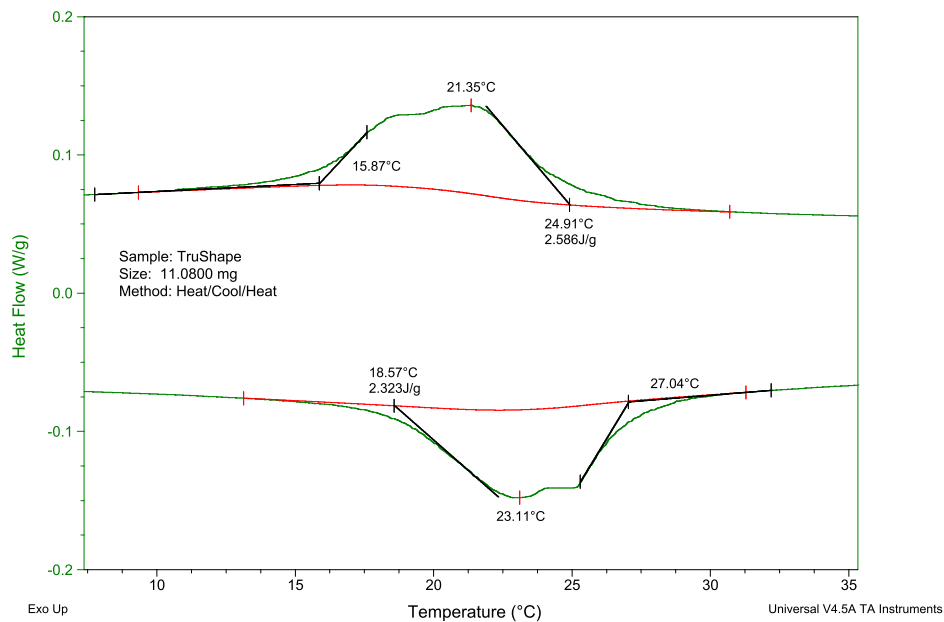


Figure 16: TRUShape, Sample 1

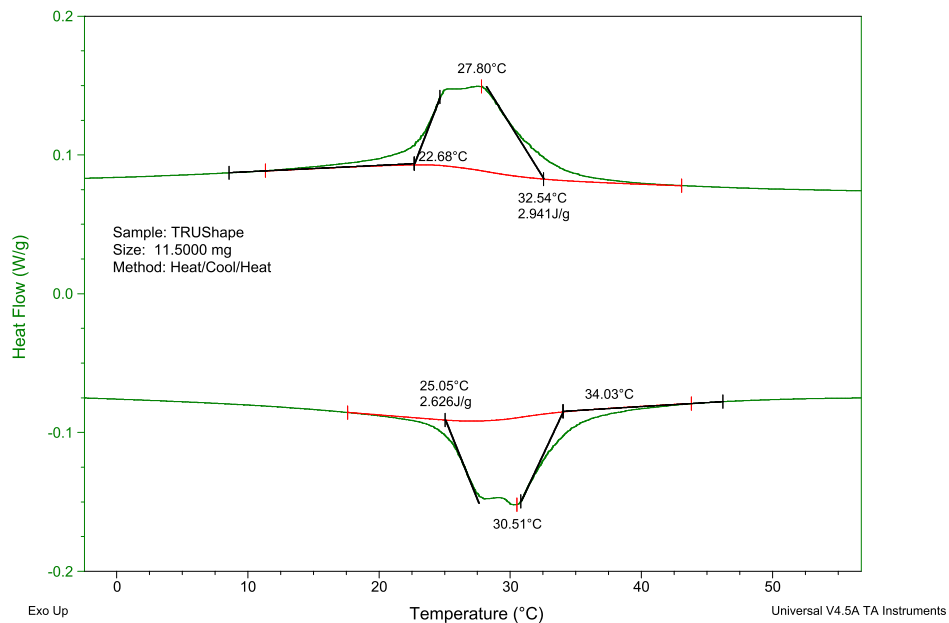


Figure 17: TRUShape, Sample 2, Cycle 1

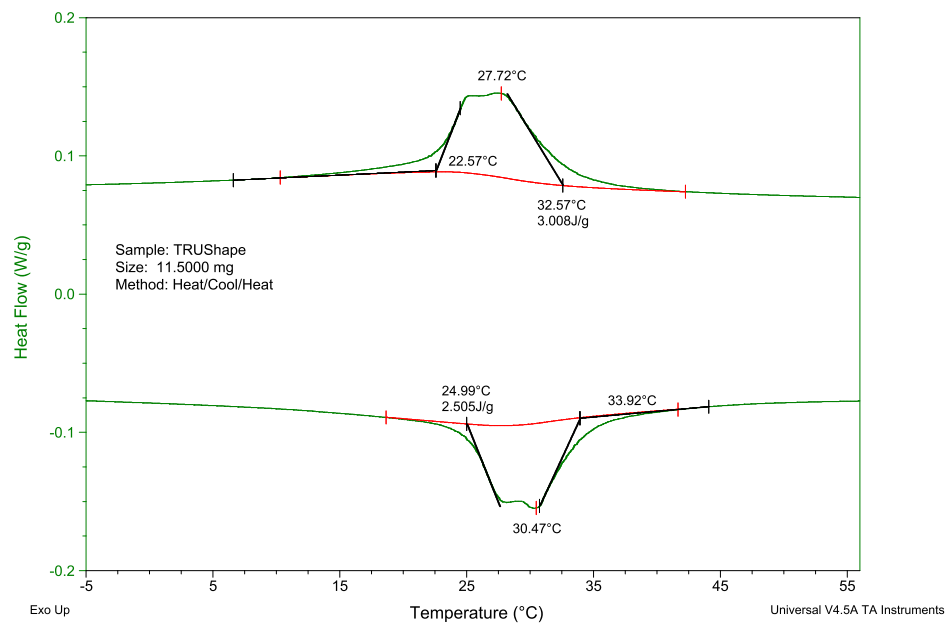


Figure 18: TRUShape, Sample 2, Cycle 2